The Seventh International Colloquium on Bluff Body Aerodynamics and Applications (BBAA7)
Shanghai, China; September 2-6, 2012

Unsteady features of bluff body wake with application to building wake length

L. Cheng, K. M. Lam*

Department of Civil Engineering, University of Hong Kong, Pokfulam, Hong Kong

ABSTRACT: This study is targeted at obtaining fluctuating characteristics of building wakes through measurement of unsteady velocity fields with time-resolved particle image velocimetry (PIV). Proper orthogonal decomposition is applied to the PIV data to identify low-dimensional substructures of the building wake. This leads to a more reliable estimation of the fluctuating ground-level length of the building wake from an instantaneous PIV snapshot. The statistics of unsteady wake lengths is important in the probability-based risk assessment of critical events of wind environment around buildings such as dispersion of hazardous pollutants, pedestrian danger and risks to aircraft landings on airport runways.

KEYWORDS: Building wake, particle-image velocimetry, proper orthogonal decomposition

1 INTRODUCTION

Wind environment around buildings has received increasing attention from researchers for a number of applications. Building wakes are known to affect dispersion of pollutants by wind. Environmental wind conditions on the pedestrian level are modified by the presence of buildings. A recent review can be found in Blocken and Carmeliet [1]. In high-rise urban areas, massive tall building developments are often accused of reducing the available wind flow to the downwind low-rise part of a city for ventilation and pollutant dispersion [2,3]. Tsang et al. [2] conducted parametric wind tunnel studies to investigate the wind environment around a group of buildings and concluded that the air movement behind the buildings is governed by the backflow created by vertical recirculation and flow passing through building separations. The relationship between these two kinds of flow determines the existence of low wind speed zones, which may impair air ventilation, and high wind speed zones, which may cause pedestrian discomfort. Yim et al. [3] studied the adverse impacts of this "wall effect" with computational fluid dynamics. The numerical results suggest that alignment of high-rise buildings leads to "wall effect" not only on air ventilation but also on pollutant dispersion rate.

Another undesirable effect of building wakes is the possible risks to aircraft landings on airport runways [4]. The objective of this study is triggered by a number of assessments of building-induced disturbance to wind flow field near runways of the Hong Kong Airport. There exist concerns about the spatial extent of building wakes causing sudden changes in wind speeds on the runways.

There have been numerous wind-tunnel and numerical investigations of wake characteristics and pollutant dispersion behaviors behind buildings of different sizes and geometries [1] but the experimental and numerical results are mostly limited to time-averaged mean wind speeds and statistical properties such as turbulence intensities. While these mean flow properties are generally useful in applications such as assessment of wind environmental conditions around tall buildings for pedestrian comforts or pollutant dispersion efficiency in downwind regions, unsteady and fluctuating flow quantities are equally important in critical situations such as dispersion of

hazardous matters and building-induced wind shear events on runways. These latter applications call for a probability approach for appropriate risk assessment and data on the fluctuating characteristics of building wakes are required. As a basic feature, it is desirable to know the maximum and minimum spatial extents of the building wake over time.

This paper reports an attempt to obtain some characteristics of fluctuating building wake through laboratory measurement. Unsteady velocities in the wake of a surface mounted bluff body are measured with time-resolved particle image velocimetry (PIV) and proper orthogonal decomposition is employed to interpolate PIV database and identify low-dimensional substructures of the building wake.

2 EXPERIMENTAL TECHNIQUES

In this study, turbulent flow behind a tall building model was measured with PIV. Fig.1 shows the schematic of the experimental arrangement. The first set of experiments was carried out in a water channel with width of 0.3 m. The target geometrical scale of the testing was 1:1000. The building model was a square-section tall building of height H = 75 mm and breadth B = 30 mm. For optical access, the building model was made of plexiglass. To simulate wind profiles over a suburban terrain, three triangular spires and 750 mm fetch of roughness elements were placed on the ground level plate upstream of the building model. Experiments were performed with the water depth 0.375 m above the ground level plate and flow velocity $U_H \approx 0.13$ m/s at the roof height of the building model. The Reynolds number was $\mathrm{Re} \approx U_H B/\nu = 4{,}350$.

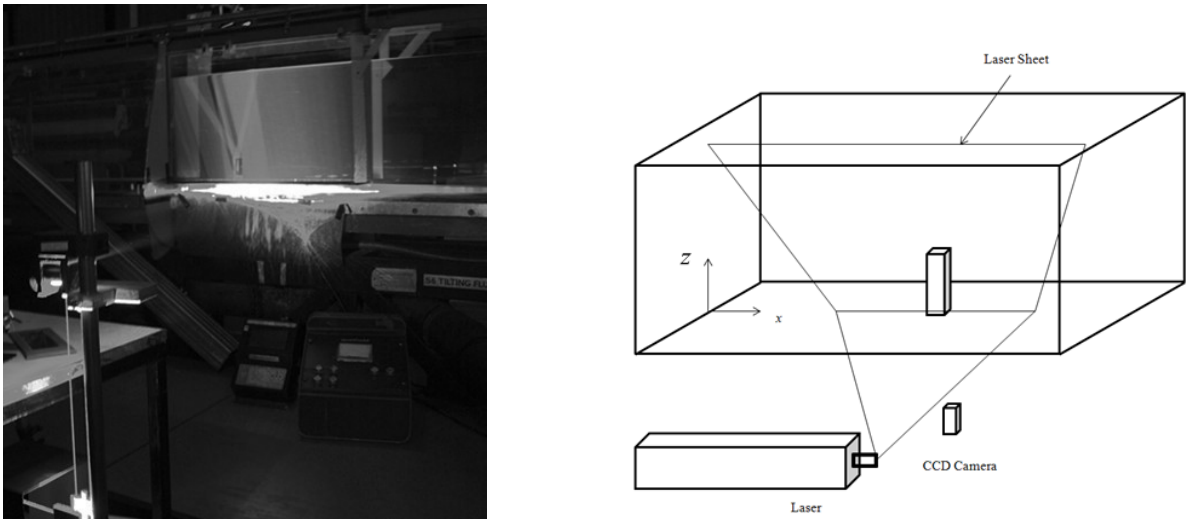

Figure 1. Experimental setup for PIV measurement.

A continuous-wave Argon-ion laser was used to generate a laser sheet to illuminate a two-dimensional plane of the flow. For flow on the central stream-wise vertical plane (x-z) of the building wake, the laser sheet was shone from below the transparent ground level plate. Neutrally buoyant polyamid particles of 35 μm nominal diameter were used to seed the water. Flow images were captured with a high speed camera (model PCO 1200hs) viewing through the transparent side window of the water channel. The camera had a resolution of 1280×1024 pixels and was set at a speed of 100 image/s to capture a time sequence of particle images of 1000-image length.

Particle images recorded on two consecutive images were analyzed for an instantaneous PIV snapshot using a PIV analysis software. The analysis was based on the spatial cross-correlation algorithm [5] but with adaptive and multi-pass interrogation windows. In the final iteration, PIV vectors were obtained on interrogation areas of size 32×32 pixels and with a 50% overlap. Thus, the two-dimensional velocity field at each time instant was consisted of 79×63 vectors of U and V.

3 POD ANALYSIS

Proper orthogonal decomposition (POD) is an efficient and elegant method of identifying lower order substructures by projecting the high-dimensional data onto a lower-dimensional space and capturing the dominant features (coherent structures) of the spatial-temporal fields with POD modes. POD is widely used in many disciplines such as image processing, signal analysis and data compression, with applications to turbulent flows starting from Lumley [6]. Kostas et al. [7] applied the snapshot POD analysis on both velocity data and vorticity data to investigate flow behind a backward-facing step at Reynolds numbers 580 and 4660. Adrian et al. [8] studied a fully developed channel flow at Reynolds number 5387 with POD analysis of PIV velocities and suggested that POD is effective at identifying the inhomogeneous spatial distribution of various eddy scales.

This study adopts the snapshot POD method [9] which solves the eigenvalue problem necessary for POD analysis in an efficient way. The implementation of POD analysis is as follows. From PIV measurement, a set of velocity components (u, v) sampled over N time steps for a period of T are obtained. First, the time-average velocity field is calculated and removed from each member of the ensemble, such as:

$$\overline{u}(x,y)=\frac{1}{N}\sum_{n=1}^{N}u(x,y,t_n)$$

The fluctuating velocity field is then given by:

$$u'(x,y,t_n)=u(x,y,t_n)-\overline{u}(x,y)$$

The two-point averaged spatial correlation function is then computed by:

$$R(x_i,x_j;y_i,y_j)=\frac{1}{N}\sum_{n=1}^{N}u'(x_i,y_i,t_n)u'(x_j,y_j,t_n)$$

The eigenvalue problem can be solved as:

$$R\Phi=\lambda\Phi$$

The N POD modes are obtained as the columns (φ) of the eigenfunctions Φ. The corresponding element of the eigenvalue vector λ defines the relative contribution of each mode to the fluctuating velocity field. Thus, the cumulative energy contribution from the first k modes is given by:

$$E_k=\sum_{i=1}^{k}\lambda_i\Big/\sum_{i=1}^{N}\lambda_i$$

After obtaining the POD modes, reconstruction of any of the original PIV snapshots can be performed using all or some of the modes as:

$$u_i(x,y,t) = a_i(t)\varphi_i$$

The coefficients $a_i(t)$ are obtained from the projection of the original data onto the POD modes:

$$\mathbf{A} = \left\langle \Phi^T, C \right\rangle$$

4 RESULTS AND DISCUSSION

The first target flow information is the fluctuating ground-level length of the building wake on the x-z plane. Figure 2 shows an example of instantaneous velocity field in the building wake from one PIV snapshot. Due to the low density of seeding particles in the wake, valid PIV velocity vectors cannot be obtained at some points. Ideally, the velocity vector map can show how wind flow over the building roof subsequently curves downwards towards the ground and the ground-level wake length can be determined by the point of reattachment. In the practical situation, the flow is highly turbulent and three-dimensional. It is difficult to trace the instantaneous streamlines and determine the wake length.

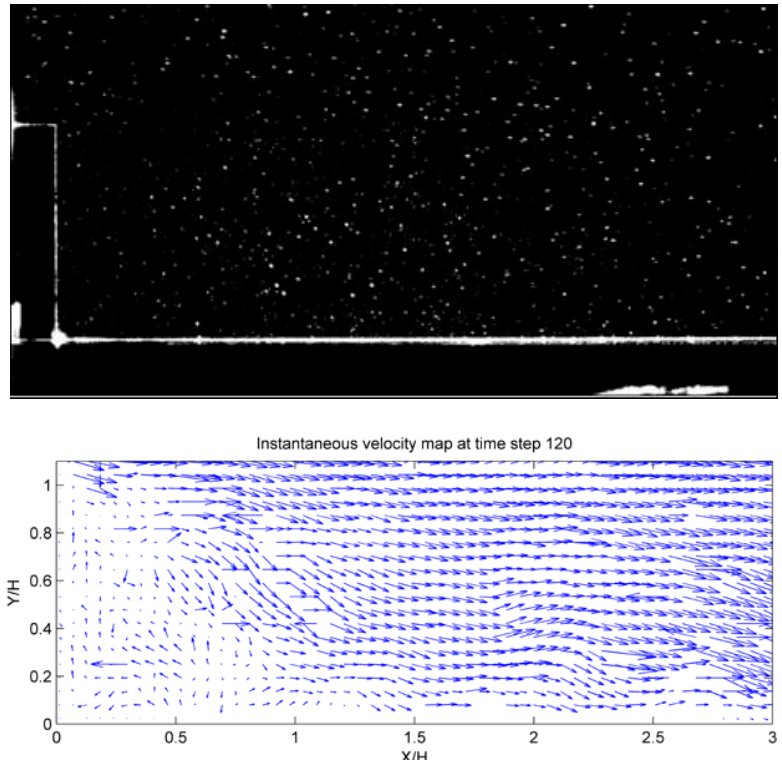

Figure 2. Example of PIV snapshot: single flow image; instantaneous velocity filed in the building wake.

The mean velocity vectors on the *x*-*z* plane averaged over all 1,000 PIV snapshots were shown in Fig. 3. The time-averaged mean flow paths and the recirculating flow behind the building are clearly revealed. However, it should be noted that this mean flow pattern will not occur at any instant along the time-axis. Figure 4 shows the axial distributions of the mean velocity component

U and the axial turbulence intensity near the ground level. The data are taken from the PIV interrogation windows closest to the ground. The mean axial velocities change from negative values inside the building wake to positive values downstream of the mean wake length. The mean building wake length is found for the change of sign at $L_w/H = 0.69$. At or very near to this location, the turbulence intensity reaches its peak value.

Figure 5 shows the velocity profiles of mean horizontal velocity components as a function of height above ground at locations upstream and downstream of the mean building wake length. Upstream of the mean building wake length, at $x/H < 0.69$, there always are some velocities having negative values. Downstream of the mean building wake length, velocities are all positive with magnitudes gradually increasing with increasing downstream distance. In other words, the mean building wake length is the location where the separation streamline from the building roof reattaches to the ground or the location where the ground-level velocities returns to the downstream direction from the reverse flow direction within the building wake.

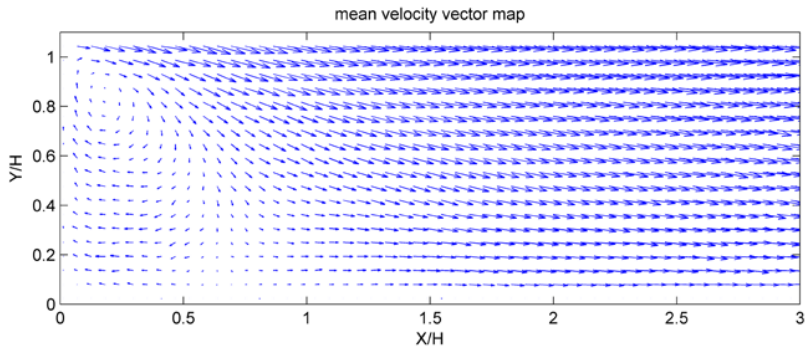

Figure 3. Mean velocity vectors on *x*-*z* plane averaged over 1,000 PIV snapshots.

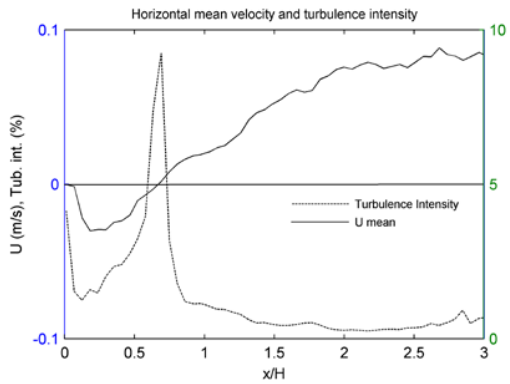

Figure 4. Mean horizontal velocity component and turbulence intensity near ground.

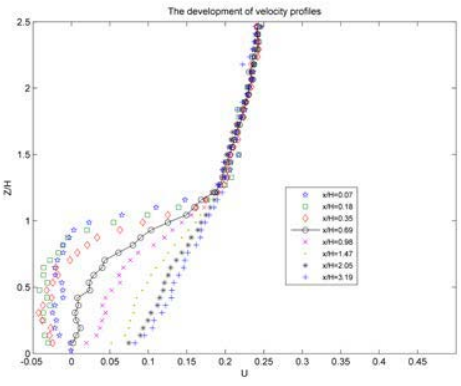

Figure 5. Profiles of mean horizontal velocities.

Attempt is made to apply the above feature to estimate the instantaneous building wake length from a PIV snapshot such as that in Fig. 2. From the instantaneous velocity vectors at any instant, the variation of horizontal velocity components along the lowest measurement points near the ground level is examined. The building wake length at that instant is determined as the length from the rear face of the building model to the location beyond which the instantaneous horizon-

tal velocities at the ground level become always positive. This is the location where the separation streamline from the building roof reattaches to the ground or the location where the ground-level velocity returns to the downstream direction from the reverse flow direction with in the building wake.

This method of wake length estimation is applied to the ensemble of 1,000 PIV snapshots. Figure 6 shows the probability density function (pdf) of the ensemble of unsteady building wake lengths. It is found that near a half of ensemble have the building wake lengths distributed over a wide range between $L_w = 0.2H$ and $1.2H$. The other half have very short wake lengths at $L_w < 0.2H$. This pdf distribution is not consistent with the feature of the mean flow pattern in Figs. 3-4. It appears that the instantaneous flow pattern consists of a number of flow structures of scales much smaller than the mean recirculating vortex. Wind flow separates on the roof leading to an unsteady shear layer behind the building model. Along the shear layer, a series of small-scale vortices are generated and this may contribute to the very small building wake lengths at some instants.

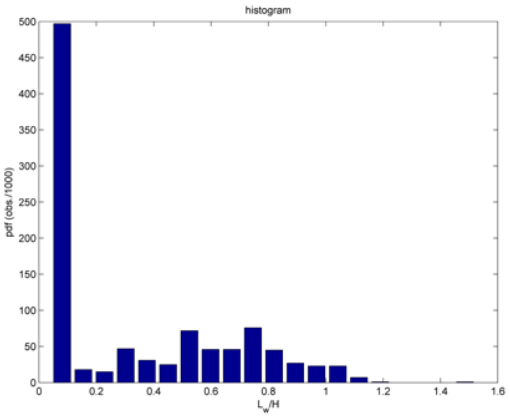

Figure 6. Histogram of building wake length of original data.

The result of Fig. 6 shows that it is not satisfactory by conducting probabilistic analysis directly with the raw velocity data. Thus, POD analysis is attempted as a potential approach in solving this problem. The two plots in Fig. 7 show the mean contours and the first five POD modes of the horizontal and vertical velocities. From the mean contour of horizontal velocity U, it can be discovered that the streamline from the top of the building reaches the ground level at the point around $x/H \approx 0.7$ and there exist some small scale turbulence before the reattachment point. In the first two U-POD modes, there exist a lot of small scale fluctuations throughout the building wake, while for modes 4 and 5 the scales of turbulent eddies become larger. In the V-POD modes, the turbulence scales are relatively larger than those in U-POD modes. Figure 8 shows that the cumulative energy of the first 50 POD modes. It is surprising to find only around 22% of the total energy is contained with these modes. The poor energy convergence may be attributed to the large variety of scales present throughout the flow. The increased level of flow complexity near the reattachment region may result in a less efficient decomposition.

Using the first 10 POD modes, the 1000 instantaneous velocity fields are reconstructed. In using only the lower modes, turbulent eddies of smaller scales are removed and only the more coherent flow eddies are retained. The unsteady building wake lengths are then estimated from these reconstructed velocity fields with the same method of ground-level horizontal velocities. Figure 9 shows the resulting pdf of the building wake lengths. The unrealistic peak at very smaller values is very much reduced and the distribution is now over a narrow range between $L_w =$

0.4H and 0.9H and with a peak at $L_w \approx 0.75H$. This peak value coincides with the mean flow patterns in Fig. 4. The original flow structure behind a building on the two-dimensional plane is complicated and upstream of the reattachment point, there exist many small-scale flow eddies behind the building. But with the reconstructed data, the small-scale structures are filtered and the reattachment point can be more easily determined. The probability distribution of L_w in Fig. 9 is valuable in the probability assessment of building wake effects such as ventilation efficiency and runway operation.

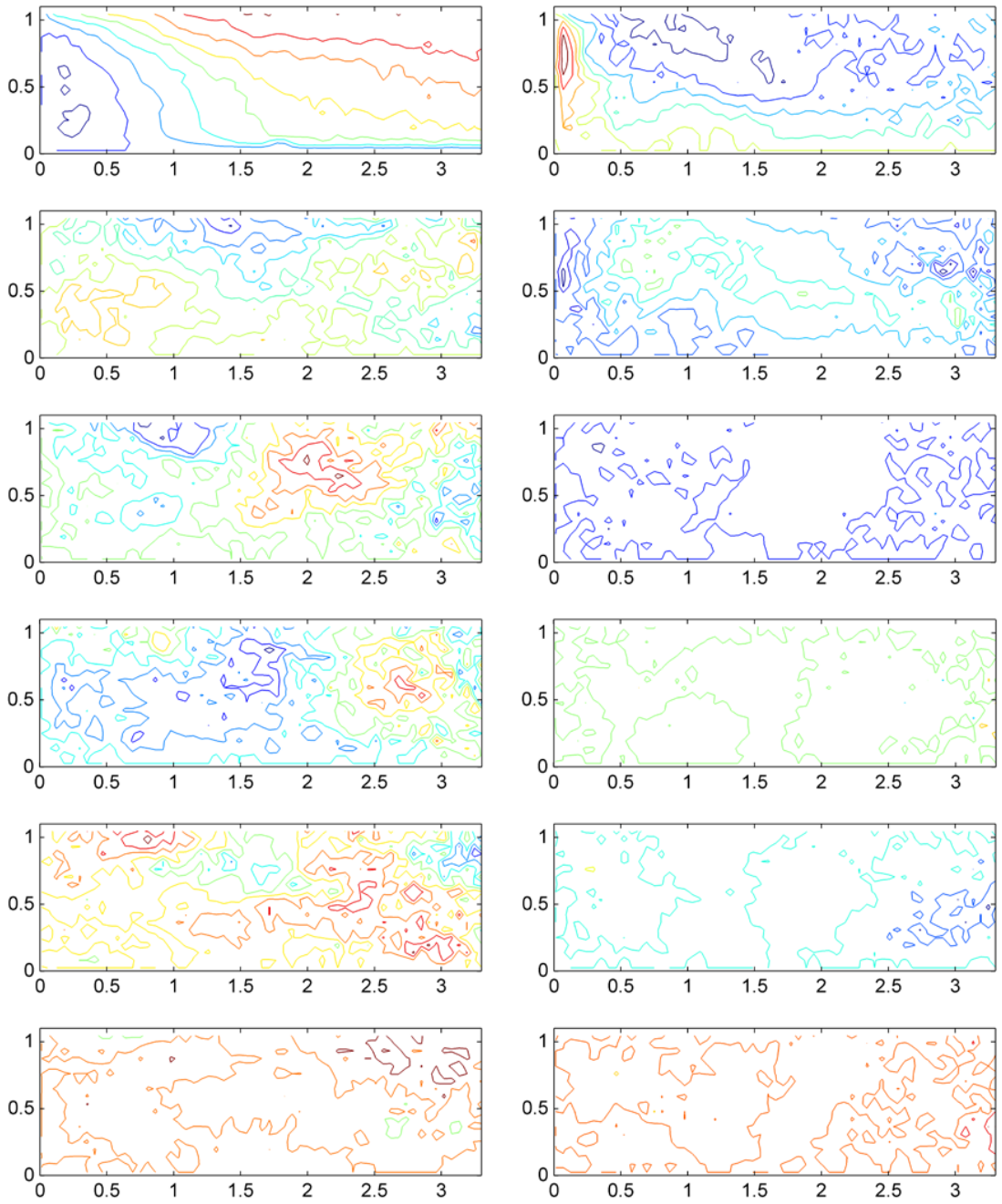

Figure 7. Mean flow and first five POD modes of horizontal (U) and vertical (V) velocities.

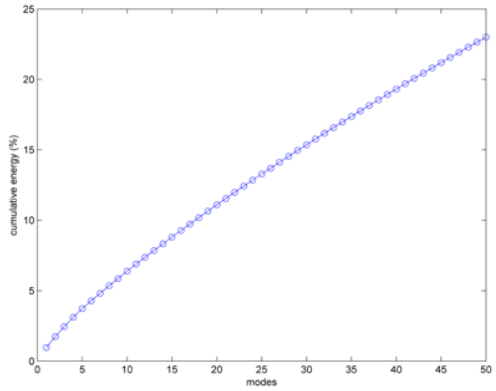

Figure 8. Cumulative energy of first 50 POD modes.

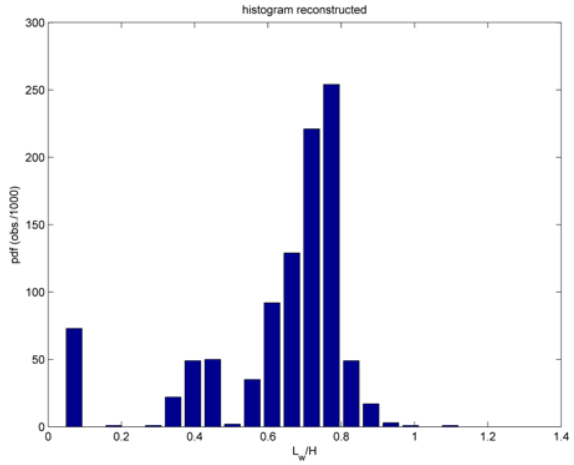

Figure 9. Histogram of building wake lengths from reconstructed data using first 10 modes.

5 CONCLUDING REMARKS

Unsteady velocity fields on the central vertical plane of a building wake are measured with time-resolved PIV in an attempt to determine some statistics of the fluctuating building wake length on the ground level. It is found that presence of small scale turbulent eddies and three-dimensionality of the flow renders estimation of the wake length from an instantaneous PIV snapshot difficult. The use of POD analysis allows filtering of small-scale flow eddies in the reconstructed velocity fields, leading to a more reliable estimation of the building wake lengths. The statistics of fluctuating characteristics of the building wake are useful in the probability-based risk assessment of critical events such as dispersion of hazardous matters and building-induced wind shear events on runways.

The Reynolds number in the reported experiments is not sufficiently high to model full-scale wind flow past a real building. More refined experiments are being carried out on building models of a larger geometric scale in a boundary layer wind tunnel. Time-resolved PIV measurements will be made to measure the unsteady flow fields on both horizontal and vertical planes in the building wake.

6 REFERENCES

[1] B. Blocken and J. Carmeliet , Pedestrian wind Environment around buildings: Literature Review and Practical Examples, J. Thermal Envelope Build. Sci. 28 (2004) 107-159.
[2] C.W. Tsang, K.C.S. Kwok and P.A. Hitchcock, Effects of building separation and podium on pedestrian-level wind environment. Proc. 7th Asia-Pacific Conf. Wind Engineering, Taipei, 2009, Paper M1B-3, 1-8.
[3] S.H.L. Yim, J.C.H. Fung, A.K.H. Lau and S.C Kot, Air ventilation impacts of the 'wall effect' resulting from the alignment of high-rise buildings. Atmos. Environ. 43 (2009)4982-4994.
[4] H.W. Krus, J.O. Haanstra, R. van der Ham and B. Wichers Schreur, Numerical simulations of wind measurements at Amsterdam Airport Schipol. J. Wind. Eng. Ind. Aerodyn. 91 (2003) 1215-1223.
[5] C.E. Willert and M. Gharib, Digital particle image velocimetry. Exp. Fluids 10 (1991) 181-193.
[6] J.L. Lumley, The structure of inhomogeneous turbulent flows. In: Atmospheric Turbulence and Radio Wave Propagation (eds. A.M. Yaglom, V.I. Tatarsky), Nauka, Moscow, 1967, 166-178.
[7] J. Kostas, J. Soria and M. S. Chong, A comparison between snapshot POD analysis of PIV velocity and vorticity data. Exp Fluids 38 (2005) 146-160.
[8] R. Adrian, K. Christensen and Z.C. Liu, Analysis and interpretation of instantaneous turbulent velocity fields. Exp Fluids 29 (2000) 275-290.
[9] L. Sirovich, Turbulence and the dynamics of coherent structures. Part 1: Coherent structures, Quart. Appl. Math. 45 (1987) 561-571.